optica

Quantum effects in the acoustic plasmons of atomically thin heterostructures: supplementary material

A. Rodríguez Echarri[1], Joel D. Cox[1,3], and F. Javier García de Abajo[1,2,*]

[1]*ICFO-Institut de Ciencies Fotoniques, The Barcelona Institute of Science and Technology, 08860 Castelldefels (Barcelona), Spain*
[2]*ICREA-Institució Catalana de Recerca i Estudis Avançats, Passeig Lluís Companys 23, 08010 Barcelona, Spain*
[3]*Center for Nano Optics and the Danish Institute for Advanced Study, University of Southern Denmark, Campusvej 55, DK-5230 Odense M, Denmark*
**Corresponding author: javier.garciadeabajo@nanophotonics.es*

10 May 2019

This document provides supplementary information to "Quantum effects in the acoustic plasmons of atomically thin heterostructures," https://doi.org/10.1364/OPTICA.6.000630. We provide here additional simulations comparing heterostructures that contain either gold or silver metallic films; simulations for structures in which the graphene is separated from the metal by hBN; the electronic band structure of gold and silver films as a function of metal thickness in the ALP model; and a plot of the function $C_g(Q)$.

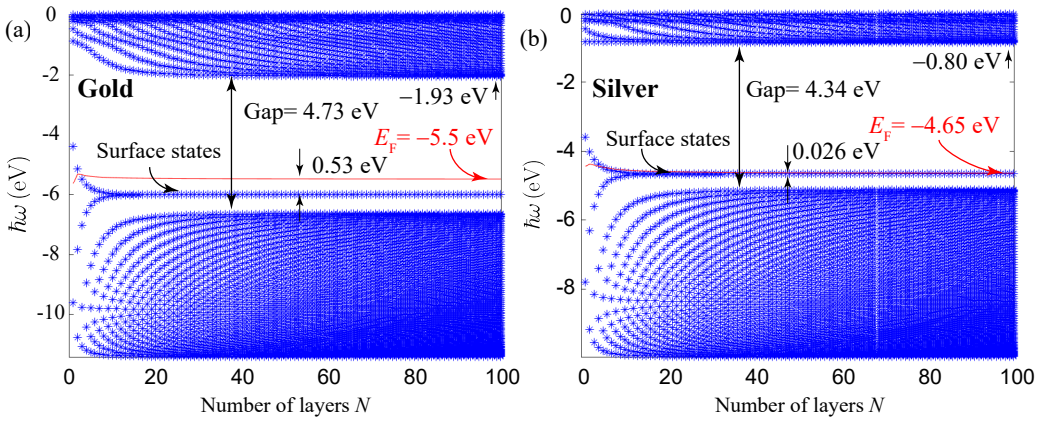

Fig. S1. Vertical electronic states of Au and Ag films as a function of thickness. Each state with zero parallel wave vector is represented by a symbol as a function of the number of atomic layers N. The dependence on parallel wave vector comes through a parabola for each of these states (not shown). The large-N-limit energies shown by labels in the plots (the Fermi energy E_F relative to vacuum, the gap energy, and the distance from E_F to the surface-state energy) reproduce the experiments in Refs. [1–3].

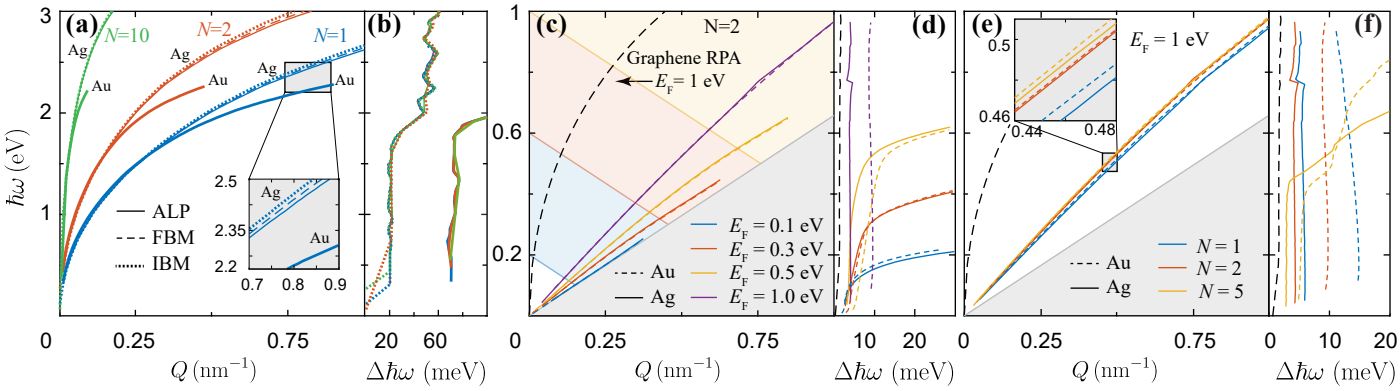

Fig. S2. Comparison of plasmons in monolayer graphene on top of atomically-thin films of either silver or gold. **(a,b)** Dispersion (a) and FWHM (b) of high-energy plasmons in films comprising N = 1-10 atomic Ag(111) layers (0.236 nm thickness per layer) obtained using the RPA. Nearly indistinguishable results are obtained by using the ALP, FBM, and IBM potentials. Results obtained from the ALP for Au (taken from Fig. 2b,c) are shown for comparison (see labels). **(c-f)** Dispersion relation (c,e) and FWHM (d,f) of acoustic plasmons in graphene-metal films containing N (111) atomic layers of gold (dashed curves) and silver (solid curves) for $N = 2$ and various graphene doping levels (c,d), and for $E_F = 1$ eV and various metal thicknesses (e,f). In (c-f) we describe graphene in the RPA and the metal using the ALP model. Results for self-standing graphene with $E_F = 1$ eV (long-dashed curves) are shown for reference.

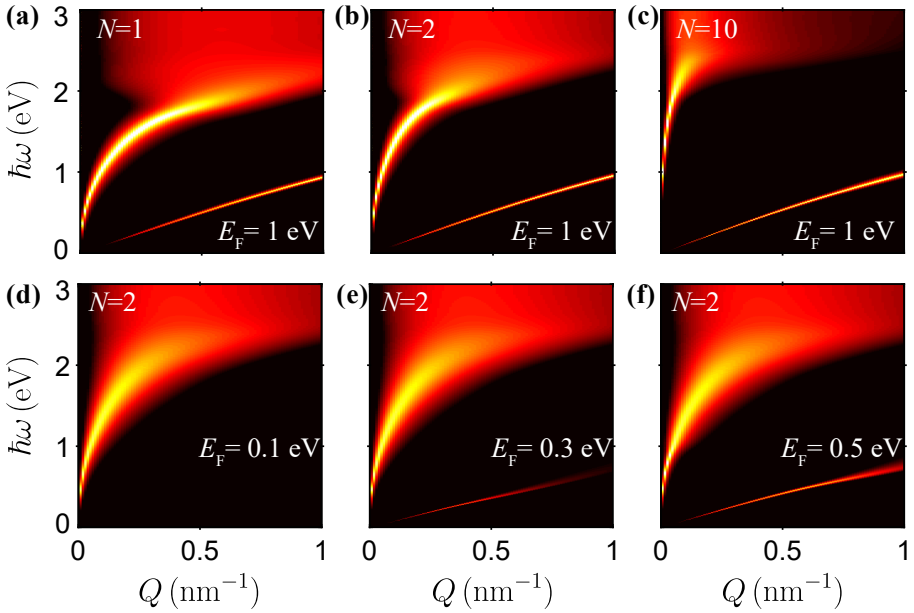

Fig. S3. Dispersion relation of graphene deposited on atomically-thin gold films. We plot the loss function $\mathrm{Im}\{R\}$, where R is the reflection coefficient (see Appendix in the main text), from which we extract the dispersion relations shown in Fig. 3b (upper plots, varying thickness N for fixed graphene doping $E_\mathrm{F} = 1\,\mathrm{eV}$) and Fig. 3d (lower plots, fixed thickness $N = 2$ for varying graphene doping E_F).

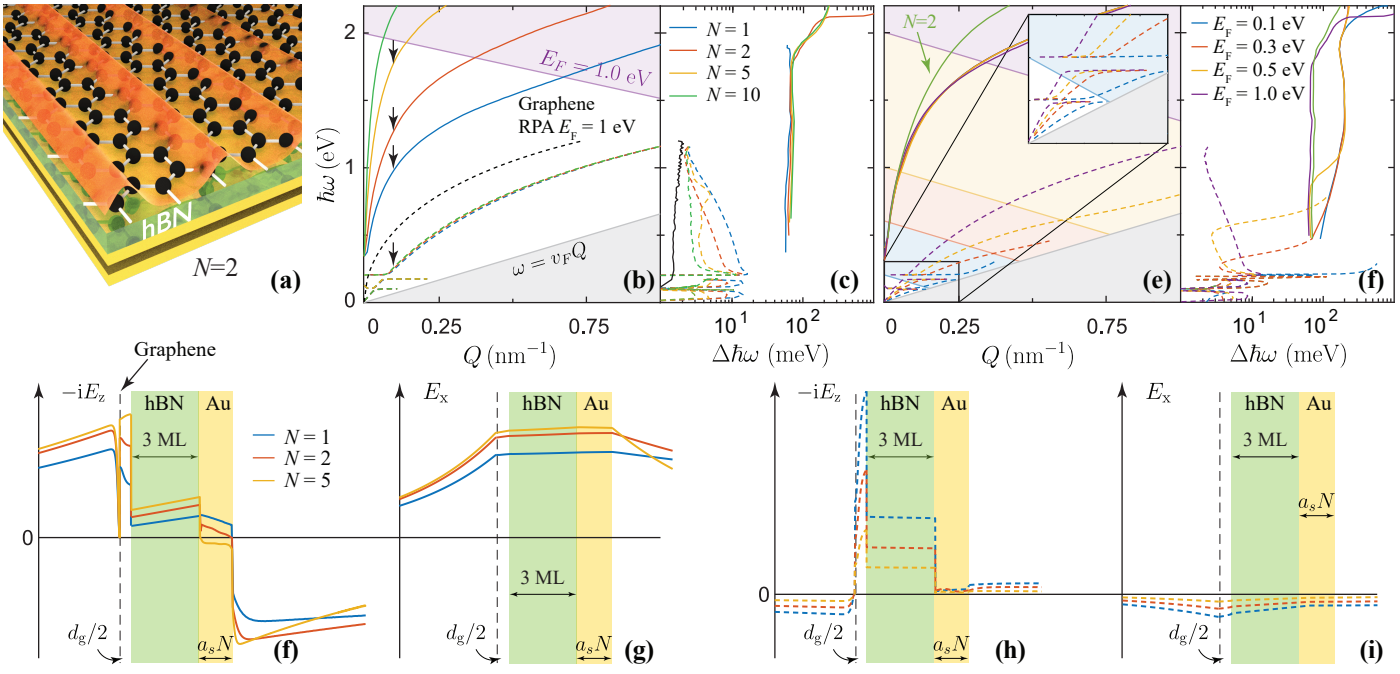

Fig. S4. Thickness and doping dependence of plasmons in graphene-BN-gold film heterostructures. Same as Fig. 3 of the main text with a layer of 1 nm of hBN (i.e., 3 MLs) separating the graphene monolayer from the metal.

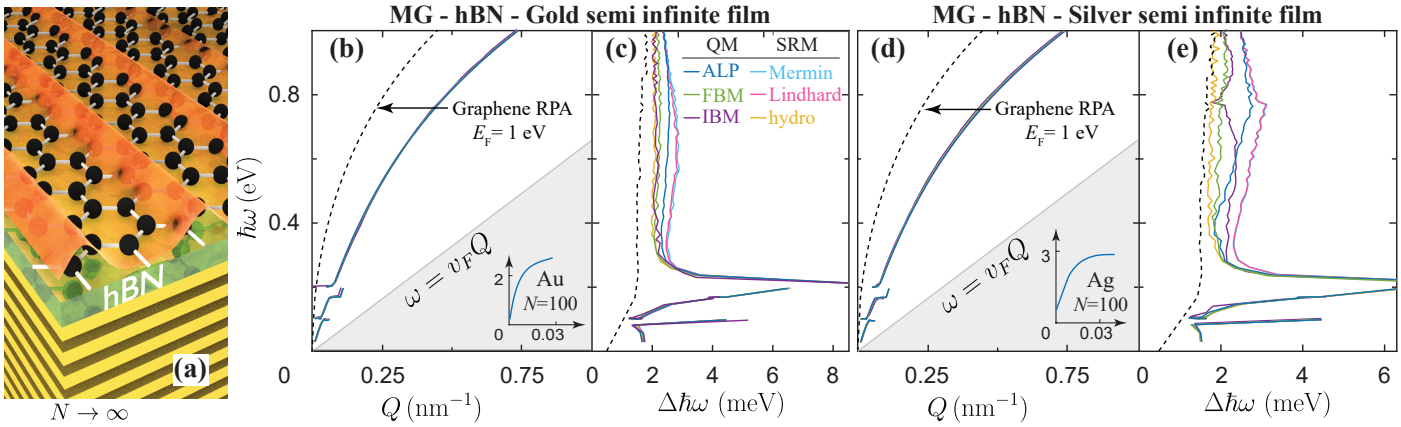

Fig. S5. Model dependence of acoustic plasmons in graphene-BN-metal hybrid films. Same as Fig. 4 of the main text with a layer of 1 nm of hBN (i.e., 3 MLs) separating the graphene monolayer from the metal.

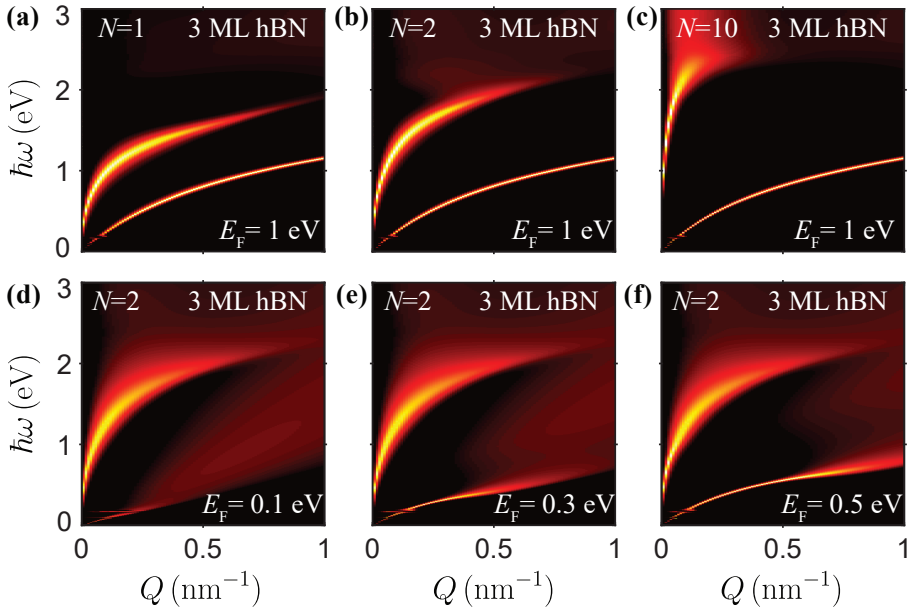

Fig. S6. Dispersion relation of graphene separated by hBN from atomically-thin gold films. We plot the loss function Im$\{R\}$ from which we extract the dispersion relations shown in Fig. S4b (upper plots, varying metal thickness N for fixed graphene doping $E_F = 1$ eV) and Fig. S4d (lower plots, fixed metal thickness $N = 2$ for varying graphene doping E_F). The intermediate hBN layer is 1 nm thick (i.e., approximately 3 ML).

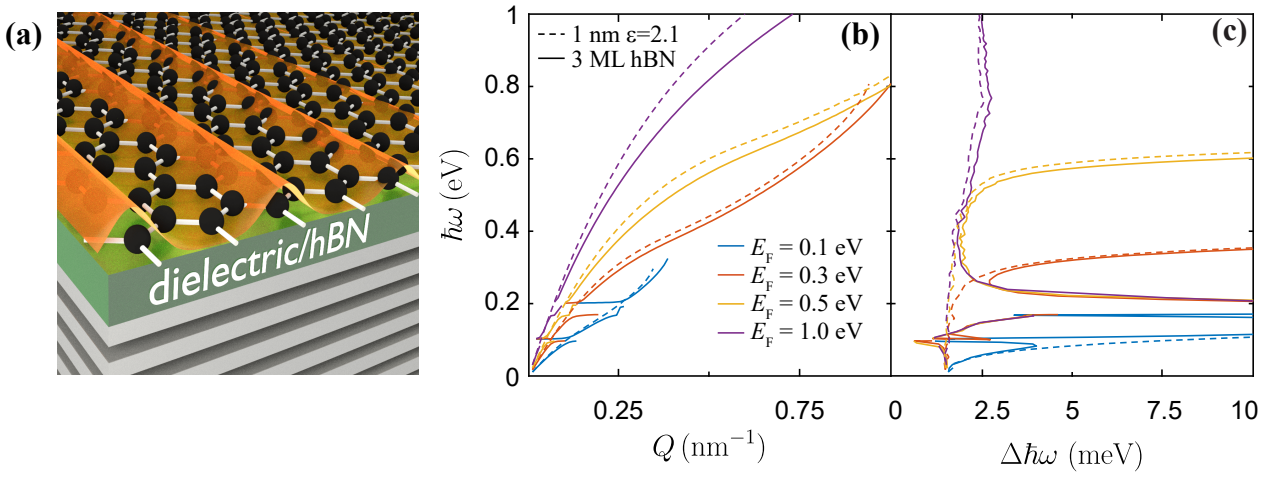

Fig. S7. Doping dependence of acoustic plasmons in a graphene-hBN-semi-inifinite silver structures. (a) Sketch of the system under consideration. The intermediate layer separating the graphene from the metal is either an isotropic dielectric ($\epsilon = 2.1$) or hBN, with a thickness of 1 nm in both cases. **(b,c)** Dispersion (b) and FWHM (c) for different graphene Fermi energies (see legend in (b)) with either an intermediate $\epsilon = 2.1$ dielectric (dashed curves) of hBN (solid curves).

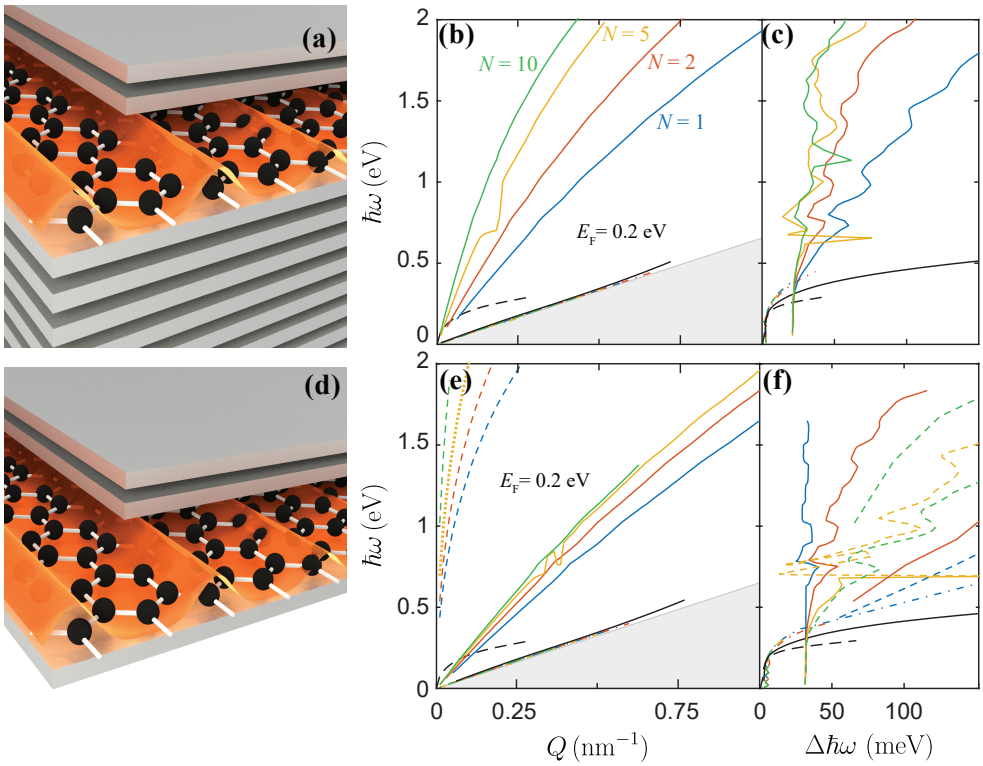

Fig. S8. Plasmons in metal-graphene-metal structures. Same as Fig. 5 of the main text with graphene doping E_F = 0.2 eV.

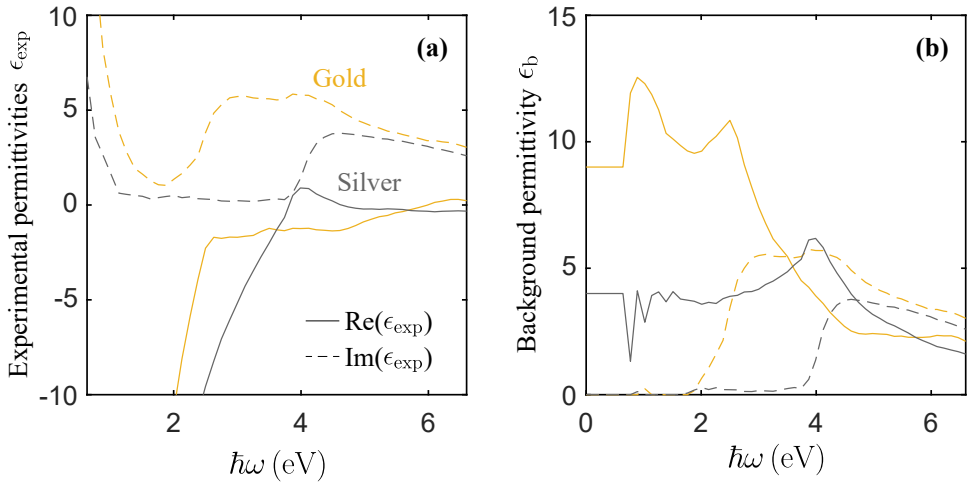

Fig. S9. Dielectric function of gold and silver. We reproduce in (a) the experimentally measured dielectric function $\epsilon_{\rm exp}(\omega)$ of Au and Ag from Ref. [4] (extrapolated as a Drude tail below 0.64 eV). In (b) we plot the background obtained by removing a Drude contribution (i.e., $\epsilon_{\rm b}(\omega) = \epsilon_{\rm exp}(\omega) + \omega_{\rm p}^2/\omega(\omega + {\rm i}\gamma)$), with parameters $\hbar\omega_{\rm p} = 9.06\,{\rm eV}$, $\hbar\gamma = 0.071\,{\rm eV}$ for Au and $\hbar\omega_{\rm p} = 9.17\,{\rm eV}$, $\hbar\gamma = 0.021\,{\rm eV}$ for Ag.

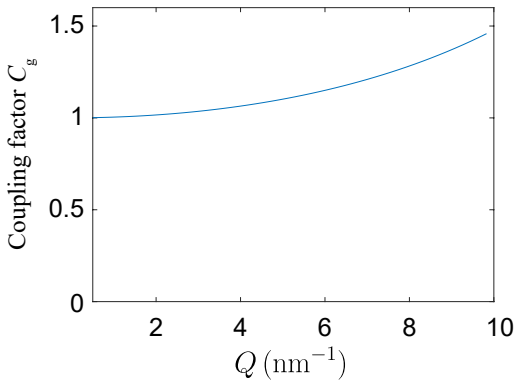

Fig. S10. Coupling factor C_g. We plot the coupling factor that accounts for the finite thickness of graphene as a function of parallel wave vector Q (see main text).

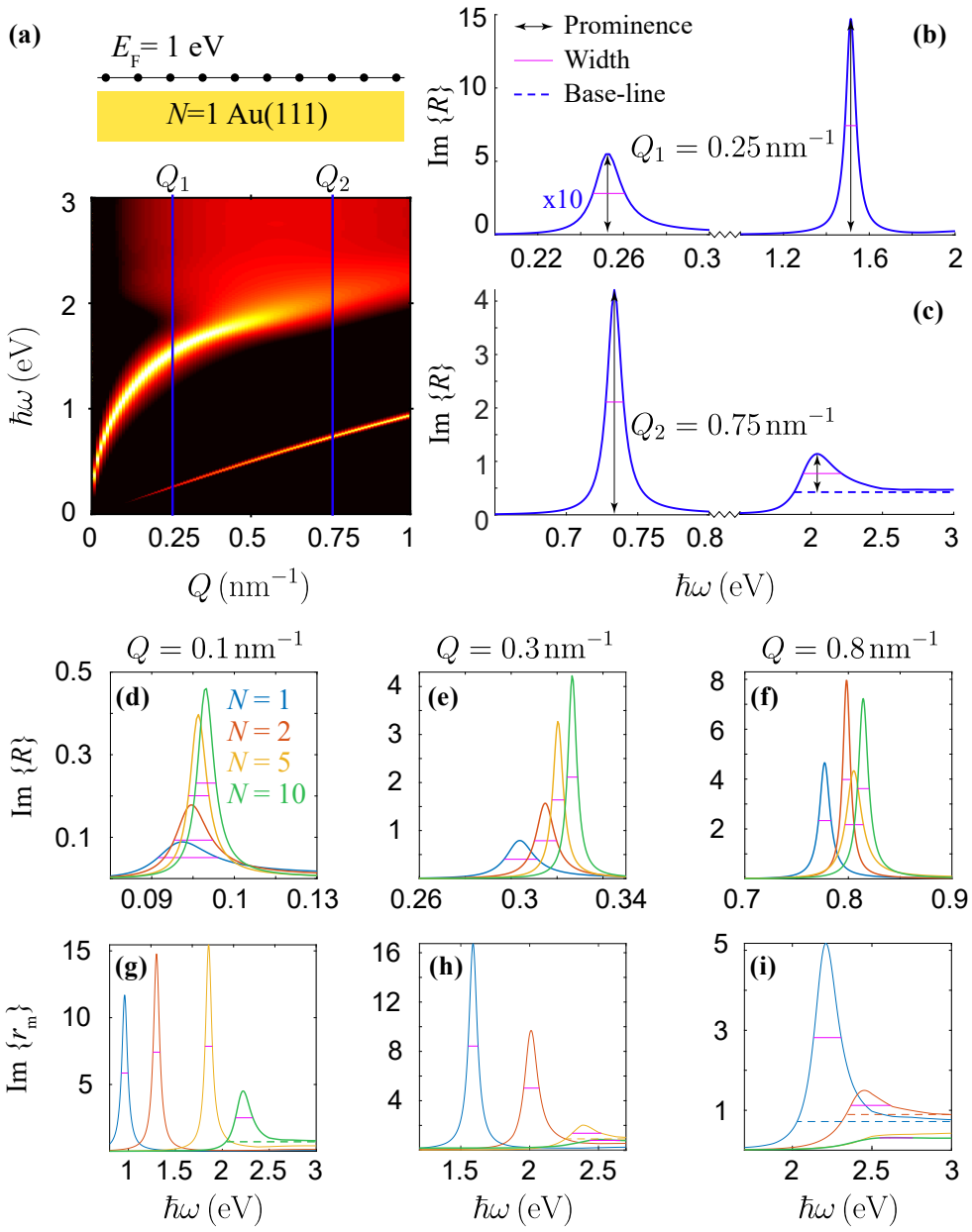

Fig. S11. Determination of the full width at half maximum (FWHM) from the calculated spectra. In this work, low-energy plasmons have well-defined Lorentzian profiles, from which the determination of the FWHM is unambiguous and does not require the subtraction of any background. However, at higher plasmon energies, the spectra become strongly asymmetric, so a background needs to be subtracted; nevertheless, this happens only when the plasmons are very lossy, so we are not interested in accurately determining their FWHM. For simplicity, we have subtracted a background obtained from the base line in the high-frequency part of the spectrum, so the FWHM is referred to the peak prominence relative to this base line. In this figure, we show several examples of this procedure, where a base line is needed when the plasmons are very lossy and their line shapes strongly asymmetric. In particular, in (b,c) we analyze the low- and high-energy plasmon branches of the system depicted in the top inset of (a) (a graphene layer with Fermi energy $E_F = 1$ eV deposited on a Au(111) monolayer) at two different values of the parallel wave vector, Q_1 and Q_2; the contour plot in (a) represents Im$\{R\}$, where R is the reflection coefficient of this hybrid structure, whereas the solid curves in (b,c) show Im$\{R\}$ along the vertical cuts indicated in (a); only the broad high-energy, high-Q plasmon in this example requires the use of a base-line subtraction (horizontal dashed line). Additionally, we plot Im$\{R\}$ in (d-f) for the acoustic plasmons in the structure considered in (a) when varying the number N of Au(111) atomic layers (see color legend in (d)); each panel corresponds to a cut of the dispersion relation in Fig. 2d of the main text at the indicated fixed values of Q. Also, in (g-i) we show the analysis of Im$\{r_m\}$ for self-standing Au(111) films (the reflection coefficient $R = r_m$ then reduces to that of the metallic film alone, r_m), corresponding to the dispersion diagrams of Fig. 2b. We use the ALP model in all simulations presented in this figure.

REFERENCES

1. S. D. Kevan and R. H. Gaylord, "High-resolution photoemission study of the electronic structure of the noble-metal (111) surfaces," Phys. Rev. B **36**, 5809 (1987).
2. E. J. Zeman and G. C. Schatz, "An accurate electromagnetic theory study of surface enhancement factors for silver, gold, copper, lithium, sodium, aluminum, gallium, indium, zinc, and cadmium," J. Phys. Chem. **91**, 634–643 (1987).
3. R. Paniago, R. Matzdorf, G. Meister, and A. Goldmann, "Temperature dependence of shockley-type surface energy bands on cu (111), ag (111) and au (111)," Surf. Sci. **336**, 113–122 (1995).
4. P. B. Johnson and R. W. Christy, "Optical constants of the noble metals," Phys. Rev. B **6**, 4370–4379 (1972).